crystals

MDPI

Article

A Combinatory Package for Diamond Anvil Cell Experiments

Yating Jia, Xin He, Shaomin Feng, Sijia Zhang, Changling Zhang, Chongwen Ren, Xiancheng Wang and Changqing Jin *

Institute of Physics, Chinese Academy of Sciences, Beijing 100190, China; jyt-1@163.com (Y.J.); hexin2018@iphy.ac.cn (X.H.); smfeng@iphy.ac.cn (S.F.); middleor@126.com (S.Z.); 18101361391@163.com (C.Z.); renchongwen@iphy.ac.cn (C.R.); wangxiancheng@iphy.ac.cn (X.W.)

* Correspondence: Jin@iphy.ac.cn

Received: 8 October 2020; Accepted: 1 December 2020; Published: 8 December 2020

Abstract: In this work, we introduce the Architecture Tech for High-Pressure Experiments Net Assembly (ATHENA) package based on diamond anvil cells, combining both the deposition of specimens as well as the detection of probes on anvils layer by layer. The specimens are typically ~1 μm in thickness and very hard to manipulate with traditional hand skills. ATHENA represents an all-in-one package by accurately synergizing chip-like networks prepared using magnetic sputtering methods and guaranteeing well-designed dimensions, positions and perfect electric contacts. We apply ATHENA successfully to the study of lanthanum metal above 60 GPa, showing very sharp pressure-enhanced superconductivity and parabolic critical temperature (Tc) evolution as a function of pressure with pressure-enhanced itinerant behavior at normal state.

Keywords: high pressure chip; all in one; diamond anvil cell

1. Introduction

High pressure is a very powerful way to change the properties of a material by modulating the interatomic spacing, electron phonon coupling, crystal structure and so on. For example, materials have shown abundant pressure-induced and novel phenomena, such as structural phase transitions, electronic topological transitions (ETT), insulator-to-metal transitions and eventually superconductivity at tens of GPa of pressure [1–8].

However, experiments with materials at very high pressure, such as at tens of GPa of pressure, are very challenging as it is necessary to load samples of several micrometers size into very small chambers. Moreover, introducing various probes or contacts to a sample with a dimension of several micrometers is very difficult to perform by hand. Although there are some reports of the production of various electric leads based on magnetic sputtering or complicated lithography techniques [8–11], the sample must eventually be loaded by hand. Here, we introduce a simple package—the Architecture Tech for High-Pressure Experiments Net Assembly (ATHENA)—that combines the deposition of both specimens and electric probes together on the anvils. The method is proven to be very effective for studying superconductivity in lanthanum (La).

2. Experimental

Figure 1 shows the schematic view of ATHENA, showing the layer-by-layer assembly of electric probes in yellow, as well as the specimen in blue. From the top to the bottom of the anvil in Figure 1, the inner electrode electrodes are shown in yellow, the blue rectangle is the sample, and the red strips are the outer electrodes. The disc between the anvils is the gasket, where the green part is composed of cBN and a central hole serves as the sample chamber.

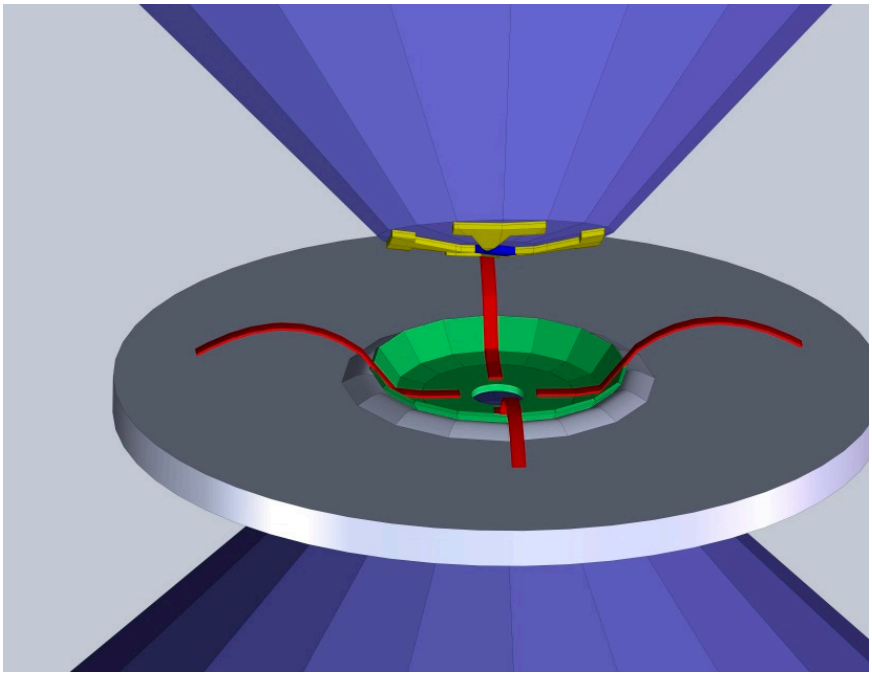

Figure 1. The schematic view of the Architecture Tech for High-Pressure Experiments Net Assembly (ATHENA) package, where red and yellow show the outer and inner electrodes, respectively, while the sample is shown in deep blue.

The shapes of both the specimen and electric probes are controlled by a mask with a specific pattern. Typically, the mask is made of gold foil of 10 μm in thickness. The pattern is fabricated by laser cutting automatically with computer-assisted design (CAD).

The Pt electrodes that serve as the inner electrodes were deposited on the surface of the culet of the upper diamond anvil with a dimension of 300 micrometers, as shown in Figure 2a. The La specimen was further deposited directly on top of the Pt electrodes of the same anvil, as shown in Figure 2b, before being clasped with the lower anvil, where the outer electrodes of 10 micrometer Au wires were located.

The size of the specimen was 60 μm (L) × 30 μm (W) × 1 μm (T), and it could be well controlled by using the mask technique during deposition. The deposition was performed with a home-fabricated magnet sputtering system with a 10^{-6} Tor vacuum. The thickness of the Pt electrodes and La specimen could be well tuned from tens of nanometers to several micrometers by changing the sputtering current and depositing time. The typical thickness was about 300 nanometers for Pt electrodes and 3 μm for La specimens in the experiments.

All the processes were conducted in a glove box with flowing Ar gas to prevent the oxidation of the La metal. The electronic transport properties of La under high pressure as a function of temperature were investigated via four probe electrical conductivity methods in a diamond anvil cell (DAC) made of CuBe alloy, as described in [8]. Pressure was generated by a pair of diamonds with a 300 μm diameter culet. A gasket made of T301 stainless steel was pressed from a thickness of 250 μm to 20 μm, and a hole was drilled at the center with a diameter of 200 μm. The hole was filled and compressed with fine cubic boron nitride (cBN) powder mixed with epoxy. A center hole of 70 μm in diameter was further drilled at the cBN layer to serve as the sample chamber. The fine cubic boron nitride (cBN) powder mixed with epoxy was pressed on the surface of the gasket to protect the electrode leads and insulate them from the metallic gasket. Au wires of 18 μm in diameter were used as the outer electrodes. The sample chamber was filled with dry NaCl powder as the pressure-transmitting medium. The pressure was determined via the ruby fluorescence method at room temperature before and after each cooling using the method described in [12]. Three ruby balls were mounted around the sample with pressure errors

of about ~2 GPa at 60 GPa. The diamond anvil cell was placed inside a MagLab system to perform the experiments. The temperature was automatically controlled by a program of the MagLab system that could provide synergetic extreme environments with temperatures from 300 K to 1.5 K and a magnetic field of up to 9 Tesla. A thermometer was mounted near the diamond in the diamond anvil cell to monitor the exact sample temperature. The X-ray diffraction (XRD) of the sample was performed on a Rigaku Ultima VI (3 KW) diffractometer using Cu Kα radiation generated at 40 kV and 40 mA. The X-ray diffraction patterns were collected with a scanning rate of 10° per minute and a scanning step length of 0.01°. The sample surface was covered with Mylar (there were no diffraction peaks for the covered materials except a background at a low-angle range) to protect samples from degradation in air. In addition to the La metal, there were also some La_2O_3 phases that we were unable to avoid during the process of the manipulation of the samples for the measurements of XRD patterns (please see the Supplementary Materials) at room temperature as La is very easy to oxidize. However, La_2O_3 is highly insulated, and thus did not contribute to the electric conductivity measurements.

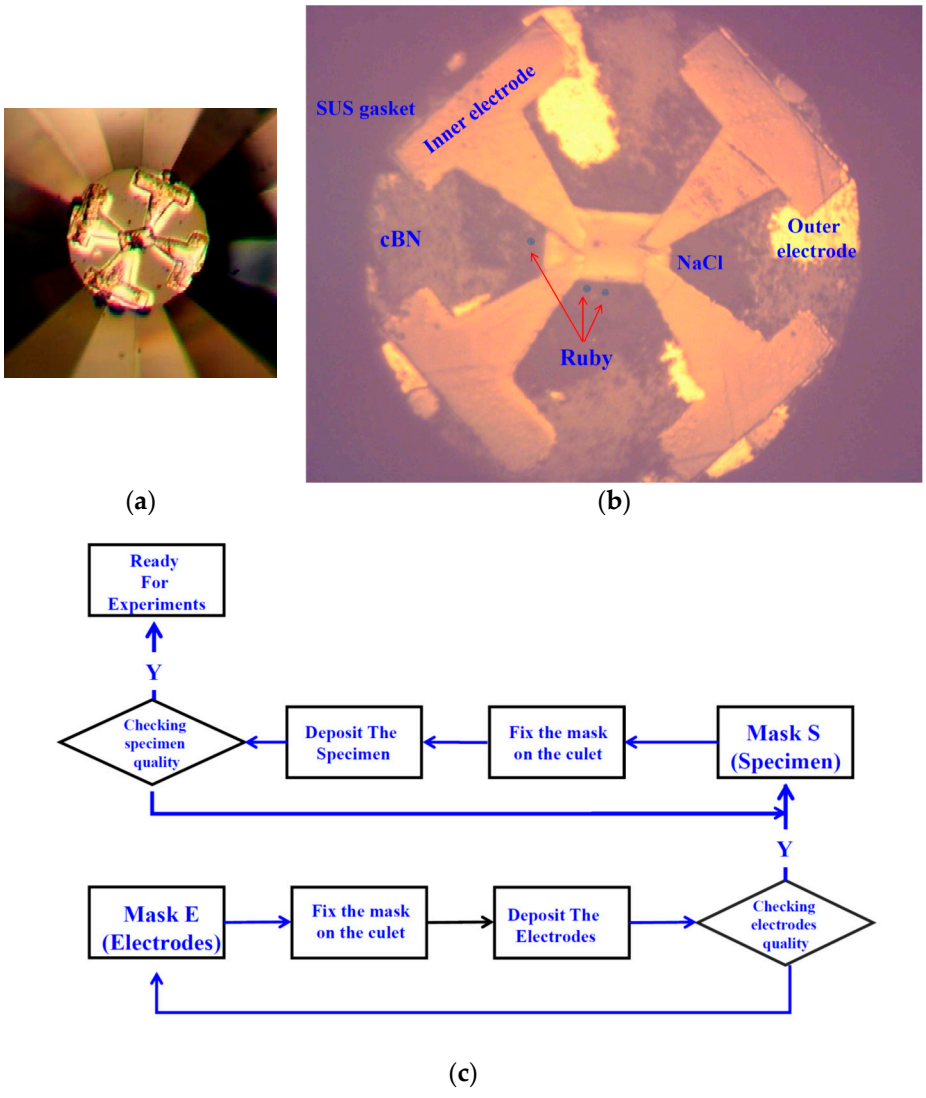

Figure 2. (**a**) The four deposited Pt electric probes that served as the inner electrodes on the culet of the diamond anvil (of 300 micrometer in size). (**b**) The La sample was further deposited above the Pt probes. The bright yellow electrodes are outer electrodes of the Au wire and the dim ones are inner electrodes, respectively. The locations of ruby balls are shown as solid circles. (**c**) The flow chart showing the primary procedure of ATHENA.

3. Results and Discussion

Figure 3a shows the evolution of resistivity (ρ) as a function of temperature for La at various pressures up to 63.3 GPa, showing very sharp superconducting transitions. La is superconductive at ambient pressure, with a critical transition temperature (Tc) of around 5 K [13]. Previous reports showed the change of Tc of La under pressure through AC susceptibility measurements. The maximum pressure previously reported was about 50 GPa [14]. The superconducting transition temperature is defined through the differentiation of ρ over temperature, as shown in Figure 3b. The temperature of onset T_c^{onset} and the temperature for zero resistivity T_c^{zero} can be easily obtained, as shown in Figure 3b. The superconducting transition width ΔT_c, which corresponds to the difference between T_c^{onset} and T_c^{zero}, is rather small (less than 1 K), as shown in the inset of Figure 3b, indicating the high quality of sample as well as a homogenous pressure environment. Hereafter, we refer to T_c^{onset} as T_c.

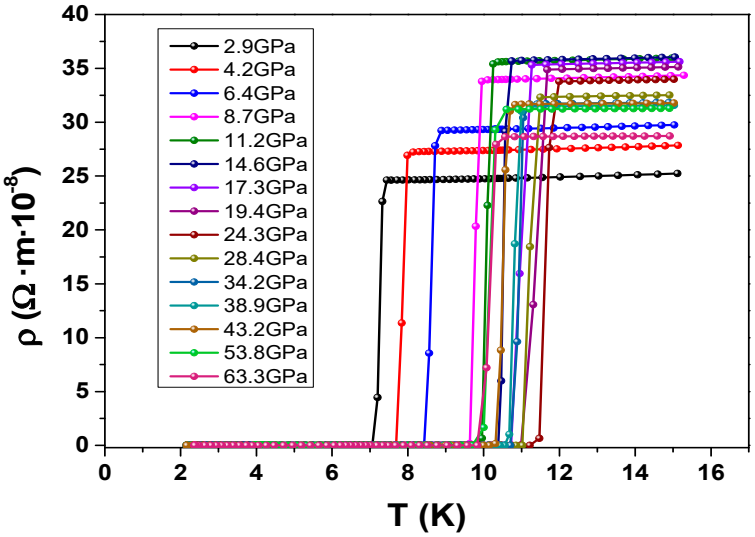

(**a**)

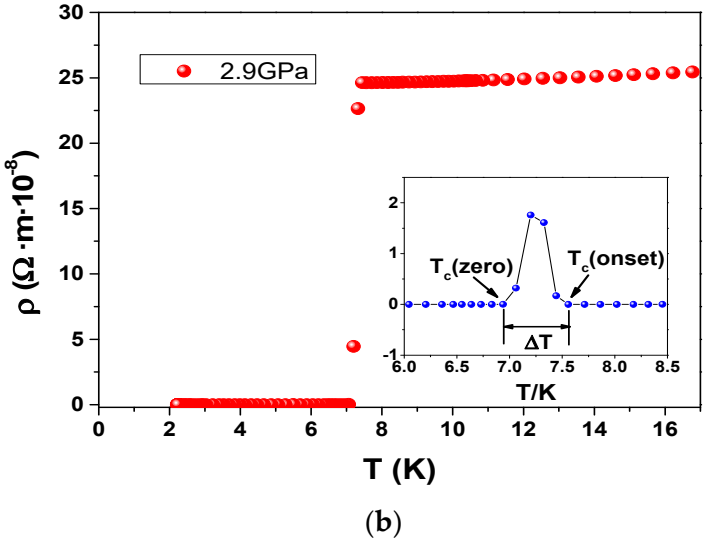

(**b**)

Figure 3. (**a**) Superconducting transition of La at various pressures, showing sharp superconducting transitions; (**b**) superconducting transition width ΔTc in terms of the width between T_c^{onset} versus T_c^{zero}, which can be well defined from the derivative of resistivity with temperature, as shown in the inset.

Figure 4 shows the evolution of T_c as a function of pressure. The T_c of La increases strongly with increasing pressure and reaches about 12 K at 24.3 GPa. Then, T_c begins to slowly decrease with a further increase in pressure. The increase in T_c up to 24.3 GPa and the subsequent fall are the result of the interplay of the interdependence among the values of the electron phonon coupling, the average phonon frequency and the Hopfield parameter [15]. We plot our results together with the previous reports in Figure 4; previous reports and experimental data are from [5,13,14], respectively. There are two structures of lanthanum at ambient conditions: (a) the stable αLa, with a double hcp (dhcp) structure; and (b) the metastable βLa, with an fcc structure. The superconducting transitions of αLa and βLa are near 5 and 6 K, respectively, at equilibrium ambient pressure. The pressure dependence of superconducting transition temperatures (Tc) of αLa and βLa metal have been reported previously. The Tc(P) of αLa shows a rather complicated variation. There is an abrupt increase in Tc near 2 GPa, and two peaks at 12 GPa and 39 GPa, respectively, as reported in [14]. The Tc of βLa increases rapidly with pressure and reaches almost 12.9 K at about 18 GPa. Thus, the evolution of Tc as a function of pressure is structure-dependent. There are two La phases in our sample, as usual—i.e., the ambient αLa and the βLa phase—as also observed in a previous report [14].

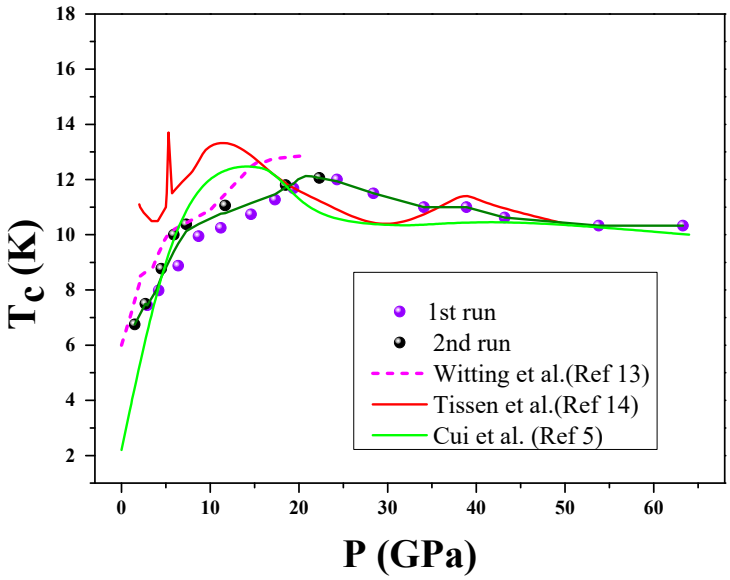

Figure 4. The evolution of superconducting transition temperature (T_c) as a function of pressure for La.

The lattice parameters for diamond and αLa are 3.56 Å and 5.32 Å, respectively, with an apparent lattice mismatch. The lattice mismatch usually results in strain. The strain can be of a GPa level sometimes and thus will affect the properties of the specimen [16]. The apparent lattice mismatch between the La specimen and diamond subtract will gives rise to compressive strain; i.e., the specimen will be at compression. This is why the high-pressure phase βLa appeared in the specimen. The βLa phase takes place at ~2 GPa, as reported in [14]. The deposition of a thin film usually causes disorder because of the rapid cooling effect, which is different from that of the bulk samples for which crystallization can be guaranteed. It is well known that disorder is harmful to the stabilization of the Cooper Pair, which is the base for superconductivity. As a consequence, the disorder will decrease the superconducting transition temperature [17]. This is the likely reason for the slightly lower Tc observed in our sample than those of the bulk samples for which the crystallization can be guaranteed studied in previous experiments. On the other hand, the experimentally observed peaks of Tc are at about 13.8 GPa, 18 GPa and 12 GPa, respectively [5,13,14]. Thus, the difference of the peak pressure of Tc can be about 6 GPa, even for previously reported bulk samples. This is reasonable if such factors as the purity or quality of samples, the nohydrostatic effects of different pressure media or the pressure calibration deviation etc. are taken into account in each experiment. Additionally, the theoretically

calculated peak of Tc is at 18.3 GPa, meaning that the lattice parameters and bulk moduli are in good agreement with experimental observations [15]. In our experiment, the peak of Tc was at ~20 GPa, which is close to the value of 18 GPa reported in [13] and the calculated value of 18.3 GPa in [15].

The dependence of Tc on pressure in our sample is generally in agreement with that of previous reports, taking into account the usual difference between film and bulk samples.

Figure 5 shows that Tc shifts at 63.3 GPa upon applying magnetic fields. A perpendicular magnetic field H was applied to the surface of the La specimen and changed from 0 Tesla to 5 Tesla with steps of 0.5 Tesla. It can be seen clearly that T_c decreases with the increasing applied magnetic field H at 63.3 GPa, indicating that the transition is superconductive. The upper critical field $H_{c2}(0)$ calculated from the Werthamer–Helfand–Hohenberg (WHH) relation of the La superconductor at 63 GPa is estimated to be 8 Tesla.

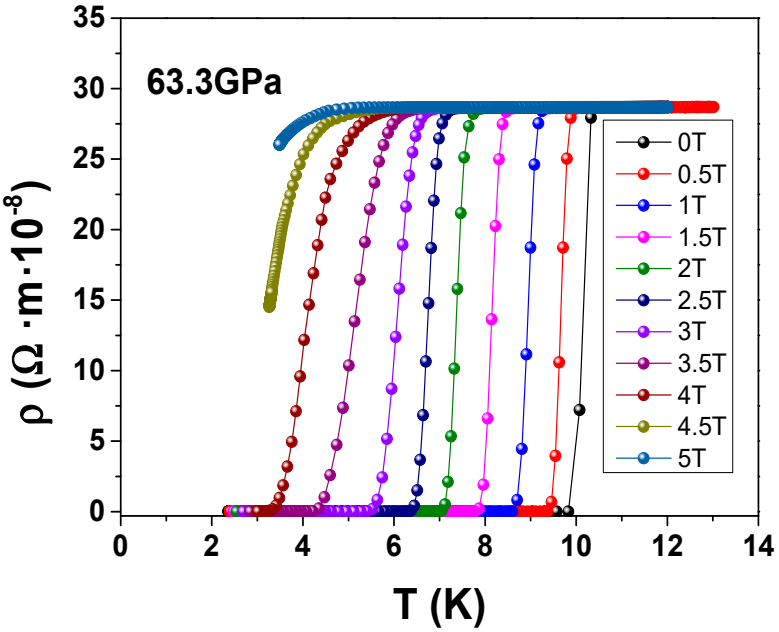

Figure 5. Temperature dependence of the resistivity at 63.3 GPa for La. The applied magnetic fields are perpendicular to the sample.

Figure 6 shows the normal state resistivity at various pressures. In order to analyze the normal state behavior under pressure, we applied the power law formula $\rho(T) = \rho_0 + AT^n$ to the resistivity of La, where ρ_0 and A are the residual resistivity and the temperature coefficient, respectively. The value of n reflects the scattering mechanism. At a low temperature, if n equals 2, it is evidence of a Fermi liquid [18]. For example, we plot the experimental curve of ρ over T at 38.9 GPa and the fitted curve in Figure 7. The fitting parameters are listed in Table 1. The adjusted R-square (degree-of-freedom adjusted coefficient of determination), which is a measure used to judge the fitting quality, is 0.99988, indicating very good reliability. Figure 8 illustrates the phase diagram of the superconducting transition temperature; normal state behavior is observed in terms of the fitted exponent n as function of pressure. The samples show superconductivity in the whole pressure range for high-pressure phases up to 63.3 GPa. The value of n moves from smaller to larger than 2 within the pressure range of experiments, indicating that normal state gradually transformed from a correlated electron system to a Fermi liquid (FL) and then to a more free electron-like system. This can be well understood as electrons become itinerant when energy bands widen at high pressures.

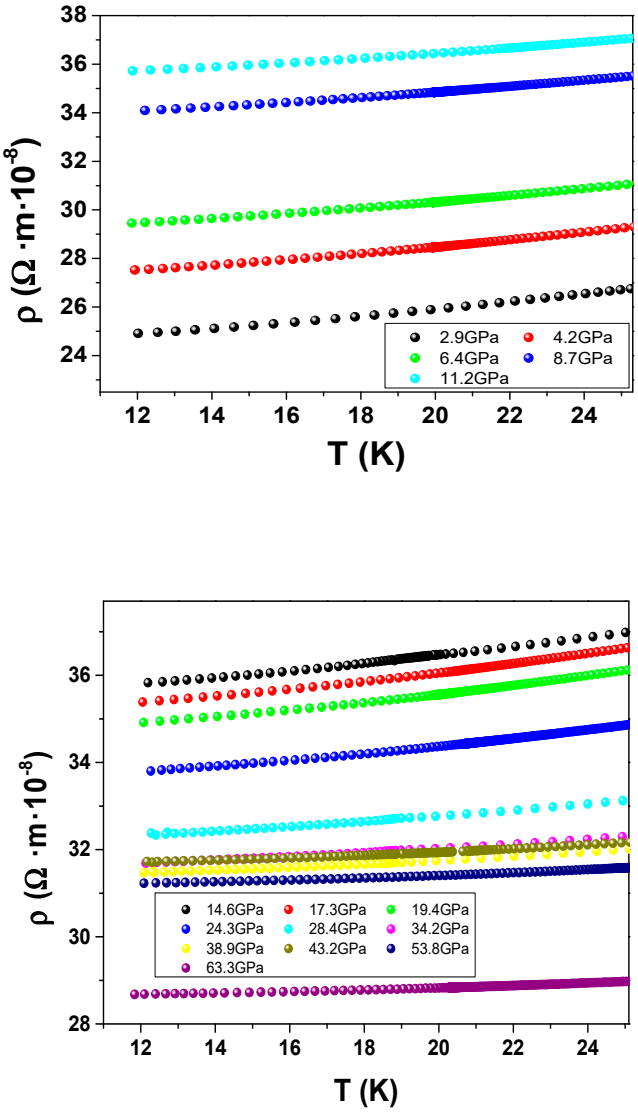

Figure 6. The resistivity under a normal state as a function of pressure.

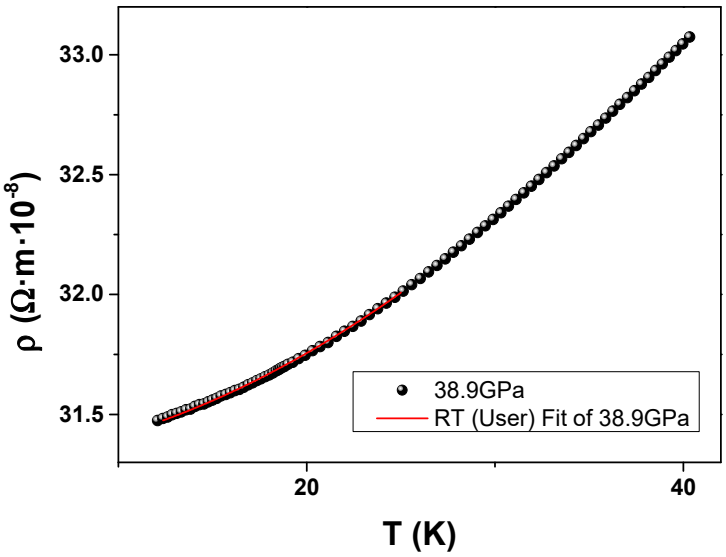

Figure 7. The fitting curve of te normal-state conductivity of La at high pressure in terms of the power law format $\rho(T) = \rho_0 + AT^n$.

Table 1. To analyze the normal state behavior under pressure, we have applied the power-law formula $\rho(T) = \rho_0 + AT^n$ to the resistivity of La, where ρ_0 and A are the residual resistivity and the temperature coefficient, respectively. The international system of units is used in the data fitting. The units of ρ, A and T are Ω·m, Ω·m·K^{-n} and K, respectively. The fitting parameters of the normal state conductivity in terms of the power law format are $\rho(T) = \rho_0 + AT^n$ at 38.9 GPa.

Equation	$\rho=\rho_0+AT^n$		
Reduced Chi-Sqr	2.67688×10^{-22}		
Adj. R-Square	0.99988		
		Value	Standard Error
C22	ρ_0	3.13431×10^{-7}	2.46144×10^{-11}
	A	5.57586×10^{-12}	3.03352×10^{-13}
	n	2.20043	0.01575

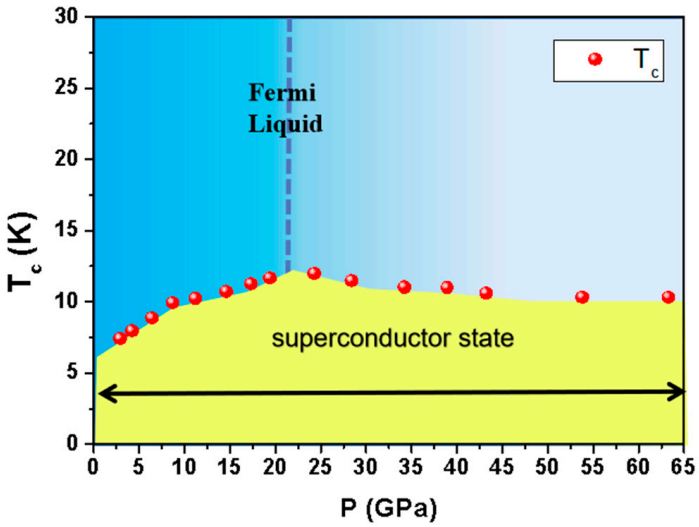

Figure 8. Superconducting phase diagram of La as a function of pressure. The dotted blue line shows the Fermi liquid behavior (n = 2) at a normal state. The normal state ranges from n~1.8 at ambient pressure to n~2.6 at 63 GPa.

4. Summary

We successfully measured the evolution of superconductivity of lanthanum as function of pressure using the Architecture Tech for High-Pressure Experiments Net Assembly (ATHENA) package based on diamond anvil cells, which combines both the preparation of a sample and electrodes in one package.

Supplementary Materials: The following are available online at http://www.mdpi.com/2073-4352/10/12/1116/s1, Figure S1: The XRD patterns of the samples at ambient pressure wherein the upper is the diffraction from the specimen while the lower are the standard patterns from αLa, βLa & La_2O_3, respectively.

Author Contributions: Conceptualization & Supervision, C.J.; Investigation, Y.J., S.Z., S.F., X.H., C.Z., X.W., C.R. & C.J.; Writing, Y.J., S.F. & C.J.; All authors have read and agreed to the published version of the manuscript.

Funding: This research was funded by the National Science Foundation and the Ministry of Science and Technology China through research projects.

Acknowledgments: The research was supported by the National Science Foundation and the Ministry of Science and Technology China through research projects.

Conflicts of Interest: The authors declare no conflict of interest.

References

1. Mao, H.-K.; Chen, X.-J.; Ding, Y.; Li, B.; Wang, L. Solids, liquids, and gases under high pressure. *Rev. Mod. Phys.* **2018**, *90*, 015007. [CrossRef]
2. Schilling, J.S. Superconductivity in the alkali metals. *High Press. Res.* **2006**, *26*, 145–163. [CrossRef]
3. Hamlin, J.J. Superconductivity in the metallic elements at high pressures. *Phys. C Supercond.* **2015**, *514*, 59–76. [CrossRef]
4. Zhu, J.; Zhang, J.L.; Kong, P.P.; Zhang, S.J.; Yu, X.H.; Liu, Q.Q.; Li, X.; Yu, R.C.; Ahuja, R.; Yang, W.G.; et al. Superconductivity in Topological Insulator Sb_2Te_3 Induced by Pressure. *Sci. Rep.* **2013**, *3*, 2016. [CrossRef] [PubMed]
5. Chen, W.; Semenok, D.V.; Troyan, I.A.; Ivanova, A.G.; Huang, X.; Oganov, A.R.; Cui, T. Superconductivity and equation of state of lanthanum at megabar pressures. *Phys. Rev. B* **2020**, *102*, 134510. [CrossRef]
6. Zhang, J.L.; Zhang, S.J.; Weng, H.M.; Zhang, W.; Yang, L.X.; Liu, Q.Q.; Feng, S.M.; Wang, X.C.; Yu, R.C.; Cao, L.Z.; et al. Pressure-induced superconductivity in topological parent compound Bi_2Te_3. *Proc. Natl. Acad. Sci. USA* **2011**, *108*, 24–28. [CrossRef] [PubMed]
7. Gao, C.; Han, Y.; Ma, Y.; White, A.; Liu, H.W.; Luo, J.; Li, M.; He, C.; Hao, A.; Huang, X.; et al. Accurate measurements of high pressure resistivity in a diamond anvil cell. *Rev. Sci. Instrum.* **2005**, *76*, 083912. [CrossRef]
8. Kong, P.P.; Sun, F.; Xing, L.Y.; Zhu, J.L.; Zhang, S.J.; Li, W.M.; Liu, Q.Q.; Wang, X.C.; Feng, S.M.; Yu, X.H.; et al. Superconductivity in Strong Spin Orbital Coupling Compound Sb_2Se_3. *Sci. Rep.* **2015**, *4*, 6679. [CrossRef] [PubMed]
9. Tsoi, G.; Stemshorn, A.K.; Vohra, Y.K.; Wu, P.M.; Hsu, F.C.; Huang, Y.L.; Wu, M.K.; Yeh, K.W.; Weir, S.T. High pressure superconductivity in iron-based layered compounds studied using designer diamonds. *J. Phys. Condens. Matter* **2009**, *21*, 232201. [CrossRef] [PubMed]
10. Welzel, O.P.; Grosche, F.M. Patterned anvils for high pressure measurements at low temperature. *Rev. Sci. Instrum.* **2011**, *82*, 33901. [CrossRef] [PubMed]
11. Hemmes, H.; Driessen, A.; Griessen, R.; Gupta, M. Isotope effects and pressure dependence of the T_c of superconducting stoichiometric PdH and PdD synthesized and measured in a diamond anvil cell. *Phys. Rev. B* **1989**, *39*, 4110–4118. [CrossRef] [PubMed]
12. Mao, H.K.; Xu, J.; Bell, P.M. Calibration of the ruby pressure gauge to 800 kbar under quasi-hydrostatic conditions. *J. Geophys. Res. Solid Earth* **1986**, *91*, 4673–4676. [CrossRef]
13. Balster, H.; Wittig, J. Pressure-induced lattice instability in fcc lanthanum at low temperature. *J. Low Temp. Phys.* **1975**, *21*, 377–414. [CrossRef]
14. Tissen, V.G.; Ponyatovskii, E.G.; Nefedova, M.V.; Porsch, F.; Holzapfel, W.B. Effect of pressure on the superconducting T_c of lanthanum. *Phys. Rev. B* **1996**, *53*, 8238–8240. [CrossRef]
15. Nixon, L.W.; Papaconstantopoulos, D.A.; Mehl, M.J. Electronic structure and superconducting properties of lanthanum. *Phys. Rev. B* **2008**, *78*, 214510. [CrossRef]
16. Schlom, D.G.; Chen, L.-Q.; Eom, C.B.; Rabe, K.M.; Streiffer, S.K.; Triscone, J.-M. Strain Tuning of Ferroelectric Thin Films. *Annu. Rev. Mater. Res.* **2007**, *37*, 589–626. [CrossRef]
17. Dubi, Y.; Meir, Y.; Avishai, Y. Nature of the superconductor–insulator transition in disordered superconductors. *Nature* **2007**, *449*, 876–880. [CrossRef] [PubMed]
18. Holmes, A.T.; Jaccard, D.; Behr, G.; Inada, Y.; Onuki, Y. Unconventional superconductivity and non-Fermi liquid behaviour of ε-iron at high pressure. *J. Phys. Condens. Matter* **2004**, *16*, S1121–S1127. [CrossRef]